

cause one NTF2 and one carrier must translocate through the NPC for each Ran cycle, the estimated minimal value for traffic through the pore is ~ 520 molecules NPC⁻¹ s⁻¹ (at 23°C).

Several predictions result from the model: (i) Ran transport is robust, suggesting that fluctuations in concentrations of transport factors can be tolerated without catastrophic cellular effects. (ii) Modulation of RCC1 activity may be a relevant mechanism for the regulation of flux in vivo. (iii) Our calculated flux rate is lower than the measured maximum transport rate in vitro (*I*), suggesting that NPC permeability is not rate-limiting within intact cells. (iv) Simulations indicate that the free RanGTP concentration is orders of magnitude lower than the dissociation constant for Ran binding to several importins (26). This suggests that our understanding of import complex disassembly is incomplete and that additional factors may be essential in vivo for cargo unloading from certain importins (27). (v) The model confirms that a steep RanGTP gradient exists across the NPC (the free RanGTP N/C ratio is ~ 500). (vi) The spatial simulations predict that steady-state cytosolic gradients also exist, likely maintained by RanGAP activity toward the RanGTP exiting the nucleus. We speculate that such gradients could provide positional information on the location of the nucleus in the cell.

References and Notes

1. K. Ribbeck, D. Gorlich, *EMBO J.* **20**, 1320 (2001).
2. J. C. Schaff, B. M. Slepchenko, L. M. Loew, *Methods Enzymol.* **321**, 1 (2000).
3. The molecular species dynamics in the model are described by a set of partial-differential equations (reaction-diffusion type), $\partial[X]/\partial t = D_x \nabla^2[X] + \sum \nu$, where $[X]$ is the concentration of species X , D_x is its diffusion coefficient, and the second term is the sum of the rates ν of the reactions affecting species X . The reversible reactions of the type $X + A \leftrightarrow AX$ [Web fig. 1 (11)] are described by mass action kinetics, $\nu = -k_{on}[X][A] + k_{off}[AX]$, where ν is the velocity, k_{on} is the forward reaction rate constant, and k_{off} is the reverse reaction rate constant. Enzyme-mediated reactions are approximated as irreversible, with Michaelis-Menten rates, $\nu = k_{cat}[E][X]/(K_m + [X])$, where $[E]$ is the enzyme concentration, k_{cat} is the catalytic-efficiency constant, and K_m is the Michaelis-Menten constant. Nuclear membrane flux densities are described: $j_x = P_x([X]_{cytosol} - [X]_{nucleus})$. Values of diffusion coefficients D_x , reaction parameters k_{on} , k_{off} , k_{cat} , and K_m , and permeabilities P_x are given in Web table 1 (11).
4. K. Ribbeck, G. Lipowsky, H. M. Kent, M. Stewart, D. Gorlich, *EMBO J.* **17**, 6587 (1998).
5. F. R. Bischoff, H. Ponstingl, *Proc. Natl. Acad. Sci. U.S.A.* **88**, 10830 (1991).
6. C. Klebe, H. Prinz, A. Wittinghofer, R. S. Goody, *Biochemistry* **34**, 12543 (1995).
7. C. Klebe, F. R. Bischoff, H. Ponstingl, A. Wittinghofer, *Biochemistry* **34**, 639 (1995).
8. K. M. Lounsbury, I. G. Macara, *J. Biol. Chem.* **272**, 551 (1997).
9. F. R. Bischoff, D. Gorlich, *FEBS Lett.* **419**, 249 (1997).
10. B. M. Paschal, L. Gerace, *J. Cell Biol.* **129**, 925 (1995).
11. Supplementary methods, tables, and figures are available on Science Online at www.sciencemag.org/cgi/content/full/295/5554/488/DC1.

12. C. Fink, F. Morgan, L. M. Loew, *Biophys. J.* **75**, 1648 (1998).
13. A. Smith, A. Brownawell, I. G. Macara, *Curr. Biol.* **8**, 1403 (1998).
14. P. R. Clarke, C. Klebe, A. Wittinghofer, E. Karsenti, *J. Cell Sci.* **108**, 1217 (1995).
15. M. Ormo et al., *Science* **273**, 1392 (1996).
16. A. E. Smith, I. G. Macara, unpublished data.
17. K. J. Zaal et al., *Cell* **99**, 589 (1999).
18. Compartmental and spatial simulations were run within Virtual Cell (2). For 3D simulations, a computational domain was decomposed into 100,860 orthogonal subvolumes (mesh size = 0.375 μ m). Equations were approximated using the finite-volume approach. The resultant system of linear algebraic equations was solved with preconditioned conjugate gradients (time steps were 10 ms long). Reversible reactions were treated as infinitely fast (2).
19. Compartmental-approximation equations transform into $\partial[X]/\partial t = F_x \equiv \sum \nu + (-1)^i J_x$ with the "flux" rate $J_x = j_x S/V_i$, where the index $i = 1, 2$ denotes cytoplasm and nucleoplasm, respectively; S is the nuclear envelope surface area; and V_i is the volume of the i th compartment. We used in simulations $S/V_2 = 0.6 \mu\text{m}^{-1}$ and $V_2/(V_1 + V_2) = 0.29$ (experimental average). Figures 2C and 4A show accumulation rates that were measured at 0.5 s.
20. V. C. Cordes, S. Reidenvach, W. W. R. Franke, *Eur. J. Cell Biol.* **68**, 240 (1995).
21. W. D. Clarkson, H. M. Kent, M. Stewart, *J. Mol. Biol.* **263**, 517 (1996).
22. K. M. Lounsbury, S. A. Richards, K. L. Carey, I. G. Macara, *J. Biol. Chem.* **271**, 32834 (1996).
23. S. A. Richards, K. L. Carey, I. G. Macara, *Science* **276**, 1842 (1997).
24. H. Nishitani et al., *EMBO J.* **10**, 1555 (1991).
25. E. Izaurralde, U. Kutay, C. Vonkobbe, I. W. Mattaj, D. Gorlich, *EMBO J.* **16**, 6535 (1997).
26. B. Senger et al., *EMBO J.* **17**, 2196 (1998).
27. L. F. Pemberton, J. S. Rosenblum, G. Blobel, *J. Cell Biol.* **145**, 1407 (1999).
28. We thank the Macara laboratory, especially M. Lindsey, M. Nemerugut, S. Plafker, K. Plafker, and A. Brownawell, and the Virtual Cell team and the Center for Biomedical Imaging Technology (University of Connecticut), especially A. Cowan, M. Terasaki, J. Carson, and J. Kirk. Supported by NIH grants GM-50526 (I.G.M.), NCR-RR13186 (L.M.L.), and NIH-GM-20438 (A.E.S.).

25 July 2001; accepted 26 November 2001

Modulation of NMDA Receptor-Dependent Calcium Influx and Gene Expression Through EphB Receptors

Mari A. Takasu,* Matthew B. Dalva,* Richard E. Zigmond,†
Michael E. Greenberg‡

Protein-protein interactions and calcium entry through the *N*-methyl-D-aspartate (NMDA)-type glutamate receptor regulate synaptic development and plasticity in the central nervous system. The EphB receptor tyrosine kinases are localized at excitatory synapses where they cluster and associate with NMDA receptors. We identified a mechanism whereby EphBs modulate NMDA receptor function. EphrinB2 activation of EphB in primary cortical neurons potentiates NMDA receptor-dependent influx of calcium. Treatment of cells with ephrinB2 led to NMDA receptor tyrosine phosphorylation through activation of the Src family of tyrosine kinases. These ephrinB2-dependent events result in enhanced NMDA receptor-dependent gene expression. Our findings indicate that ephrinB2 stimulation of EphB modulates the functional consequences of NMDA receptor activation and suggest a mechanism whereby activity-independent and activity-dependent signals converge to regulate the development and remodeling of synaptic connections.

During the development of the central nervous system, patterned neuronal activity drives the specification and maturation of synaptic connections (1, 2). The NMDA-type excitatory glutamate receptor regulates these activity-dependent processes in part by controlling the entry of Ca²⁺ into neurons, which then activates signaling pathways that orchestrate neuronal development (3). Prior to the development of synapses, young neurons differentiate and begin the process of axon growth and guidance by a mechanism that is largely independent of neuronal activity (4). The molecular mechanisms that allow activ-

ity-dependent processes to build upon activity-independent cues are not clear.

The ephrins and their receptors, the Eph tyrosine kinases, are cell-surface proteins that play a role in mediating the initial interaction between axons and dendrites as well as other activity-independent processes during neural development (5, 6). The Eph receptor proteins are classified into the EphA and EphB families on the basis of their preference for binding of glycosyl-phosphatidylinositol-linked ephrinA ligands or transmembrane ephrinB ligands, respectively. At the time of synaptogenesis, EphBs are localized to the

postsynaptic region of excitatory synapses, suggesting a role for EphBs in synaptic function (7, 8). In cultured neurons, ephrinB binding of EphB promotes the interaction of EphB with NMDA-type glutamate receptors (9), suggesting that EphB receptor tyrosine kinases might modulate NMDA receptor function.

We investigated whether ephrinB2 activation of EphB could modulate Ca^{2+} conductance through the NMDA receptor. To assay for changes in the concentration of intracellular Ca^{2+} ($[Ca^{2+}]_i$), we incubated cultured cortical neurons from embryonic day 18 (E18) rats with the Ca^{2+} indicator dye fura-2-AM (10). Although these neurons expressed NR1 and NR2B receptor subunits and responded to membrane depolarization, treatment of these neurons with glutamate (20 to 40 μ M) to activate the NMDA receptor in the presence of inhibitors of the L-type Ca^{2+} channel (nimodipine) and the AMPA-type glutamate channel (6-cyano-7-nitroquinoxaline-2,3-dione; CNQX) resulted in only a small increase in $[Ca^{2+}]_i$ (Fig. 1A) (11).

Division of Neuroscience, Children's Hospital, and the Department of Neurobiology, Harvard Medical School, 300 Longwood Avenue, Boston, MA 02115, USA.

*These authors contributed equally to this work.
 †Present address: Department of Neurobiology, Case Western Reserve University School of Medicine, 10900 Euclid Avenue, Cleveland, OH 44106, USA.
 ‡To whom correspondence should be addressed. E-mail: michael.greenberg@tch.harvard.edu

This suggests that in cultured embryonic neurons, NMDA receptor subunits are expressed before synapse formation, but are not yet fully functional. We considered the possibility that ephrinB/EphBs might enhance the ability of the NMDA receptor to regulate the influx of Ca^{2+} . Cultured cortical neurons were exposed to activated ephrinB2-Fc, a fusion protein consisting of the extracellular domain of ephrinB2 fused to the Fc portion of human immunoglobulin G1 that is multimerized with antibodies to cluster and activate EphB. Neurons were assessed for changes in $[Ca^{2+}]_i$ in response to glutamate stimulation. EphrinB2 treatment followed by glutamate stimulation resulted in a large increase in $[Ca^{2+}]_i$ (Fig. 1, A and B). The increase in glutamate-stimulated $[Ca^{2+}]_i$ in ephrinB2-treated cultures required the NMDA receptor, because the NMDA receptor antagonist 2-amino-5-phosphonovalerate (D-APV) blocked this increase in $[Ca^{2+}]_i$ (Fig. 1C).

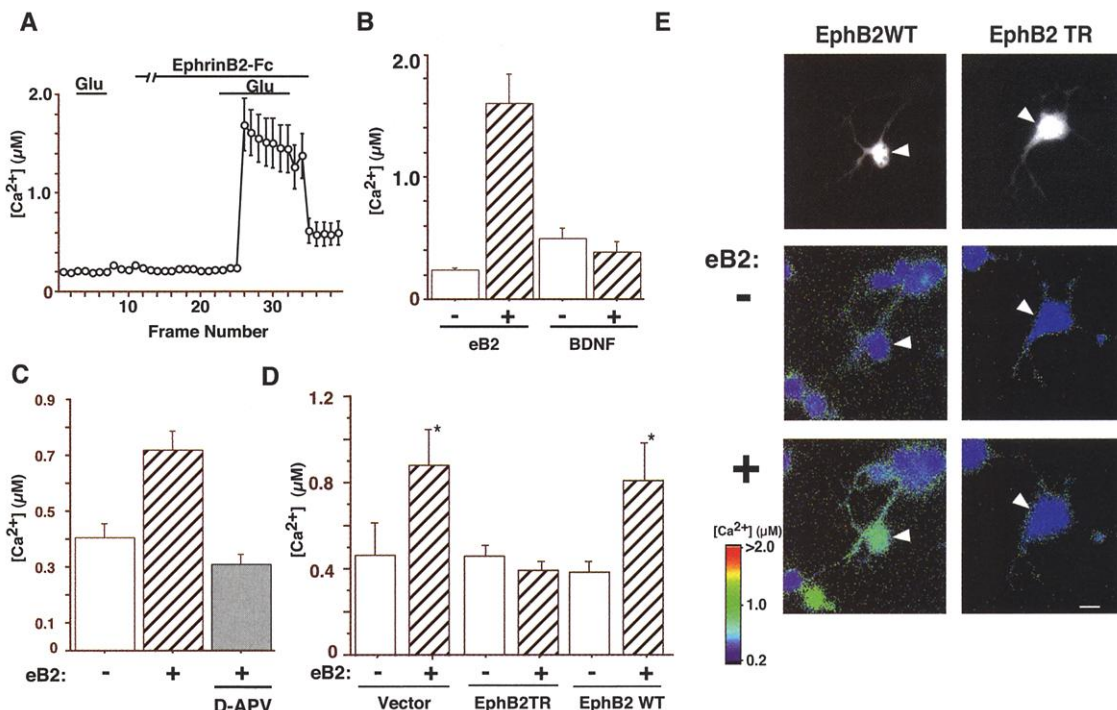
To determine whether the ephrinB2 effect is selective for the NMDA receptor, we depolarized neurons with 55 mM KCl to trigger Ca^{2+} influx through voltage-sensitive Ca^{2+} channels before and after ephrinB2 treatment. EphrinB2 treatment had no effect on Ca^{2+} influx caused by membrane depolarization, even when the depolarization stimulus was submaximal (11). Unlike ephrinB2, Fc alone or brain-derived neurotrophic factor (BDNF), which activates the trkB receptor tyrosine kinase, did not result in an increase in gluta-

mate-stimulated $[Ca^{2+}]_i$ (Fig. 1B) (11).

EphrinB binding activates the EphB receptor tyrosine kinase and promotes its association with cytoplasmic proteins that mediate the effects of receptor activation (12). We thus investigated whether the cytoplasmic domain of EphB2, including the tyrosine kinase domain, is required for the ephrinB2 potentiation of NMDA receptor-dependent Ca^{2+} influx (10). In neurons transfected with either vector control (pCDNA3) or an EphB2 wild-type construct (EphB2WT), glutamate-stimulated NMDA receptor-mediated Ca^{2+} influx was increased after ephrinB2 treatment (Fig. 1, D and E). However, in neurons expressing an EphB2 construct containing a deletion of the EphB2 cytoplasmic domain (EphB2TR) (9), ephrinB2 treatment did not cause an increase in glutamate stimulation of NMDA receptor-dependent Ca^{2+} influx (Fig. 1, D and E). Thus, the cytoplasmic region of EphB2 is required for the increase in glutamate-stimulated Ca^{2+} influx through the NMDA receptor.

Tyrosine phosphorylation of the modulatory NR2 subunits of the NMDA receptor occurs both during development as well as in paradigms of synaptic plasticity, and can regulate NMDA receptor channel properties (13–17). In our cortical culture system, NR2B is the predominant NR2 subunit expressed (18, 19). To examine NR2B tyrosine phosphorylation, we stimulated cultured cortical neurons with aggregated ephrinB2-Fc or Fc, immunoprecipitated

Fig. 1. EphrinB2 activation of EphB enhances glutamate-stimulated Ca^{2+} influx through the NMDA receptor. (A) Trace of average $[Ca^{2+}]_i$ during Ca^{2+} imaging for E18 + 1 DIV cultured cortical neurons in the presence of nimodipine and CNQX ($n = 30$ cells). Neurons were stimulated with glutamate (40 μ M; Gibco-BRL), washed with artificial cerebrospinal fluid, treated with ephrinB2-Fc for 40 min, and again stimulated with glutamate. (B) $[Ca^{2+}]_i$ in response to glutamate stimulation before (–) and after (+) treatment with ephrinB2-Fc (eB2) or BDNF was quantified [$*P < 0.01$ versus (–), analysis of variance (ANOVA); $n = 30$ cells per condition]. (C) Neurons were treated as in (A) and then stimulated with glutamate in the presence (+) or absence (–) of the NMDA receptor antagonist D-APV (10 μ M; RBI), and $[Ca^{2+}]_i$ was compared [$*P < 0.01$ versus (–), ANOVA; $n = 13$ cells per condition]. (D) Average $[Ca^{2+}]_i$ in E18 + 1 DIV neurons overexpressing pCDNA3 (vector), EphB2TR, or EphB2WT in response to glutamate stimulation before (–) and after (+) ephrinB2 treatment was compared [$*P < 0.01$ versus (–), ANOVA;



$n = 10$ cells, pCDNA3; $n = 11$ cells, EphB2WT; $n = 32$ cells, EphB2TR]. (E) Representative examples of neurons transfected with either EphB2WT or EphB2TR and GFP and visualized by fluorescence microscopy (top panels) and by fura-2-AM labeling after glutamate stimulation (30 μ M) before (–) and after (+) treatment with ephrinB2-Fc.

REPORTS

NR2B from neuronal lysates with antibodies to NR2B (anti-NR2B), and monitored tyrosine phosphorylation of the immunoprecipitated protein using anti-phosphotyrosine, PY99 (20). EphrinB2 treatment of neurons increased tyrosine phosphorylation of NR2B (Fig. 2A). When we expressed an expression construct for NR2B with either a wild-type EphB2 construct (WT) or an EphB2 mutant that lacks kinase activity (VM and KR) in human embryonic kidney (HEK) 293T cells, we found that NR2B became tyrosine phosphorylated only when coexpressed with EphB2WT (Fig. 2B), suggesting that EphB2 kinase activity or a kinase that associates with activated EphB is important for the ephrinB2-stimulated increase in NR2B tyrosine phosphorylation.

We also transfected into HEK293T cells an expression vector encoding EphB2 along with a vector encoding wild-type NR2B, or NR2B mutants in which tyrosines in the terminal 400 amino acids of the cytoplasmic tail of NR2B

were converted to phenylalanines (20). This mutational analysis and the subsequent generation of phospho-specific antibodies to putative sites of tyrosine phosphorylation revealed that when EphB2 and NR2B are expressed together, NR2B becomes tyrosine phosphorylated on tyrosines 1252, 1336, and 1472 (Fig. 2C). To determine whether phosphorylation of NR2B at 1252, 1336, and 1472 by EphB2 affects Ca²⁺ flux through the NMDA receptor, we expressed NR1 together with NR2BWT or NR2B mutated at tyrosines 1252, 1336, and 1472 (NR2BTM) and EphB2WT or kinase-dead EphB2 (EphB2VM) in HEK293T cells. Stimulation of cells expressing NR1, NR2BWT, and EphB2WT with 0.04 μM glutamate resulted in a robust increase in Ca²⁺ influx, whereas in the absence of EphB2, with expression of EphB2VM, or expression of NR2BTM, the Ca²⁺ response was significantly lower (Fig. 2D). These results suggest that phosphorylation of NR2B at tyrosines 1252, 1336, and 1472 is

required for the EphB2-mediated enhancement of Ca²⁺ influx through the NMDA receptor.

These three tyrosines on NR2B are phosphorylated by Fyn, a member of the Src family of tyrosine kinases (21). Members of the Src family physically associate with both EphB and NMDA receptors, and Src family members can modulate the open time of the NMDA receptor channel (13, 17, 22, 23). We thus considered the possibility that ephrinB binding to EphB activates a Src family member, which would then phosphorylate NR2B, thereby enhancing the ability of the NMDA receptor to conduct Ca²⁺ upon glutamate stimulation. We treated cultured cortical neurons at E18 + 1 DIV with aggregated ephrinB2-Fc, Fc, or BDNF, which is known to activate Src family members, and assessed Src activation using an antibody specific for phospho-Tyr⁴¹⁶, because phosphorylation of Tyr⁴¹⁶ occurs when Src is activated (20, 24). EphrinB2 treatment of neurons led to an increase in the amount of Src that was phosphorylated at Tyr⁴¹⁶ (Fig. 3A), and to an inducible interaction between EphB2 and Src (19). Although BDNF treatment also activates Src, BDNF does not alter glutamate-stimulated Ca²⁺ influx and, in contrast to ephrinB2, leads to NR2B tyrosine phosphorylation at sites other than 1252, 1336, and 1472 (Fig. 1B) (19, 25, 26). These findings suggest that ephrinB2 treatment leads to the selective localization and activation of Src and to NR2B tyrosine phosphorylation.

We used two small molecule inhibitors of the Src family of tyrosine kinases, PP2 and SU6656, to assess the importance of Src activation for ephrinB2-induced NR2B phosphorylation. Both PP2 and SU6656, but not PP3, the inactive analog of PP2, inhibited the ephrinB2-induced increase in NR2B tyrosine phosphorylation in neurons (Fig. 3B). Also, expression of EphB2 and NR2B in HEK293T cells with a dominant inhibitory Fyn construct (FynDN), which inhibits activation of Fyn and other Src family members, inhibited NR2B tyrosine phosphorylation (19). These findings suggest that ephrinB2 binding to EphB leads to the activation of a Src family member that in turn phosphorylates NR2B. An EphB2 mutant (EphB2-EE) that is catalytically active but cannot bind Src family members (27) did not promote tyrosine phosphorylation of NR2B (Fig. 3C). Thus, EphB activation of Src family members is required for the effects of ephrinB2 on tyrosine phosphorylation of the NMDA receptor.

We used dominant inhibitory and constitutively active Fyn constructs (FynDN or FynCA, respectively), EphB2EE, or the Src inhibitor PP2 to determine whether Src family members are required for ephrinB-dependent potentiation of Ca²⁺ influx through the NMDA receptor. Overexpressing FynDN, EphB2EE, or treatment with PP2 prevented the ephrinB2-induced increase in NMDA receptor-dependent [Ca²⁺]_i (Figs. 2D and 3, D and E). These findings

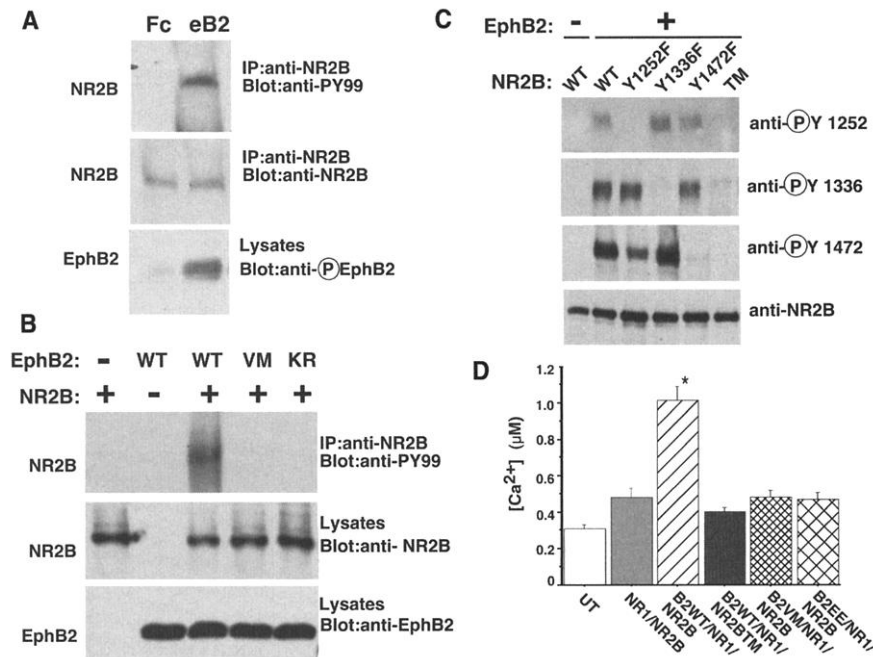


Fig. 2. Increased tyrosine phosphorylation of the NMDA receptor after ephrinB activation of EphB. (A) Effect of ephrinB2-Fc treatment on NR2B tyrosine phosphorylation. Cortical neurons at E18 + 1 DIV were stimulated with ephrinB2-Fc or Fc and then lysed, and NR2B was immunoprecipitated with anti-NR2B. Western analysis was performed with anti-phosphotyrosine (PY99; Santa Cruz), anti-NR2B (NR2B; Affinity Bioreagents), or anti-phospho-EphB2 (*n* = 6). (B) Role of EphB2 protein kinase activity in NR2B tyrosine phosphorylation. HEK293T cells were transfected with NR2B alone, EphB2WT alone, NR2B and EphB2WT, or NR2B and catalytically inactive EphB2 constructs (EphB2VM or EphB2KR). Lysates were analyzed as in (A) and immunoblotted with anti-phosphotyrosine, anti-NR2B, or anti-EphB2 (*n* = 3). (C) Sites of NR2B tyrosine phosphorylation by EphB2. HEK293T cells were cotransfected with EphB2 and various NR2B constructs: NR2BWT, NR2B mutated at single tyrosines to phenylalanine (NR2BY1252F, Y1336F, Y1472F), or the triple mutant [(TM)Y1252F/Y1336F/Y1472F]. Western analysis was performed with antibodies that specifically recognize phosphorylated tyrosines 1252, 1336, or 1472 on NR2B (*n* = 3). The antibody to phosphotyrosine (PY99) does not detect tyrosine phosphorylation of NR2BTM or NR1 when these constructs are coexpressed with EphB2WT. (D) Role of NR2B tyrosine phosphorylation for glutamate-dependent Ca²⁺ influx. Average [Ca²⁺]_i in HEK293T cells expressing NR1 together with NR2BWT, or NR2BTM, and either EphB2WT, EphB2VM, or EphB2EE stimulated with 0.04 μM glutamate [**P* < 0.01; untreated (UT), *n* = 30; NR1/NR2B, *n* = 16; B2WT/NR1/NR2B, *n* = 73; B2VM/NR1/NR2BTM, *n* = 55; B2VM/NR1/NR2B, *n* = 59; B2EE/NR1/NR2B, *n* = 20]. The expression levels of EphB2, NR1, and NR2B were verified by Western blot. Untransfected (non-GFP-labeled) cells did not respond to glutamate.

REPORTS

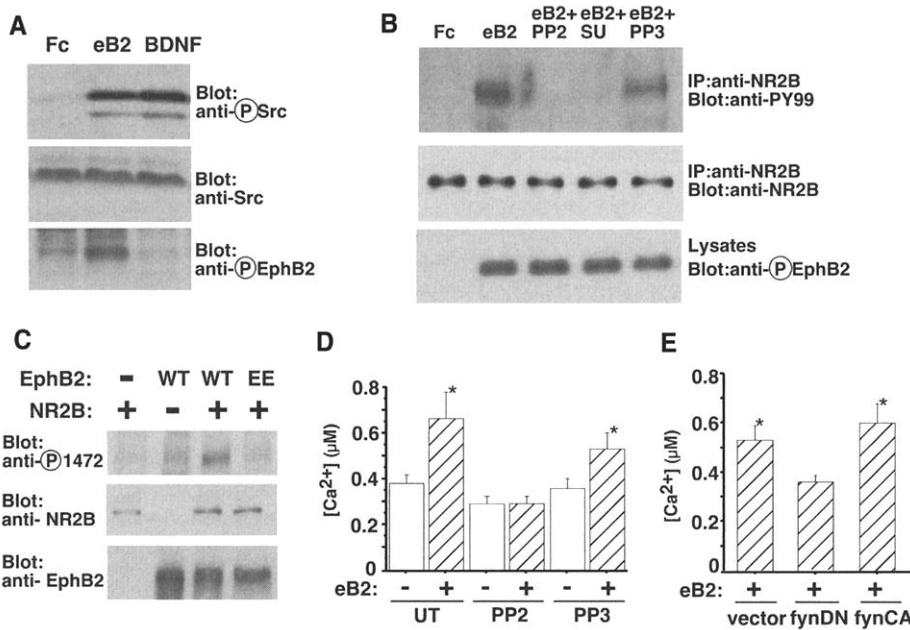


Fig. 3. Requirement of Src tyrosine kinase family members to mediate the effects of ephrinB2 treatment. **(A)** Effects of ephrinB2 stimulation on the activity of Src family members. Cortical neurons at E18 + 1 DIV were stimulated with Fc, ephrinB2-Fc, or BDNF, and Western analysis was performed with anti-Src phospho-Tyr⁴¹⁶ (BioSource International), anti-Src (UBI), or anti-phospho-EphB2 (*n* = 3). **(B)** The role of Src family members in NR2B tyrosine phosphorylation. Neurons were treated with PP2, PP3, or SU6656 at 0.5 μ M and analyzed as in Fig. 2A (*n* = 6). **(C)** HEK293T cells were cotransfected with NR2B alone, EphB2WT alone, NR2B and EphB2WT, or NR2B and EphB2EE, and lysates were analyzed by Western blot with anti-NR2B phospho-Tyr¹⁴⁷², anti-NR2B, or anti-EphB2 (*n* = 3). **(D)** Role of Src family members in glutamate-stimulated Ca²⁺ influx. Neurons were treated with PP2 (0.5 μ M) or PP3 (0.5 μ M), and the effect of glutamate-stimulated [Ca²⁺]_i before (–) and after (+) ephrinB2 treatment was quantified [**P* < 0.01 versus (–) and untreated (UT), ANOVA; *n* = 18 cells per condition]. **(E)** Average [Ca²⁺]_i in neurons overexpressing pCDNA3, FynDN, or FynCA following glutamate stimulation after (+) ephrinB2 treatment

(**P* < 0.01 versus before ephrinB2 treatment, ANOVA; *n* = 9 cells, pCDNA3; *n* = 30 cells, fynDN; *n* = 9 cells, fynCA).

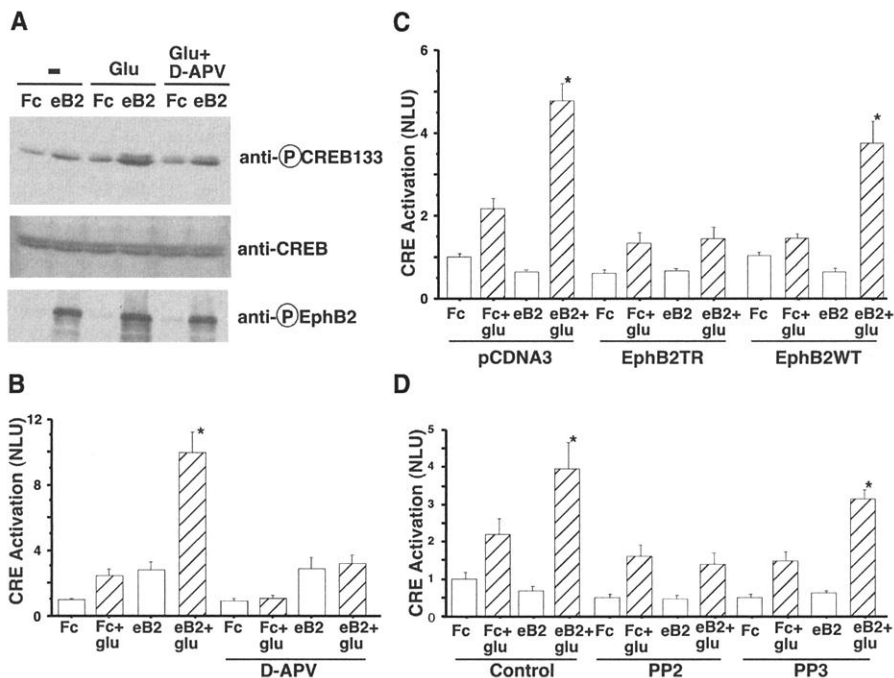


Fig. 4. Potentiation of CREB-dependent transcription after EphB activation. **(A)** Effect of ephrinB2 treatment on CREB Ser¹³³ phosphorylation. Lysates from neurons treated with ephrinB2-Fc or Fc before glutamate stimulation (20 μ M; 10 min) were immunoblotted with anti-CREB phospho-Ser¹³³, anti-CREB, or anti-phospho-EphB2 (*n* = 5). Neurons were first treated with D-APV (10 μ M) to block NMDA receptors (*n* = 2). EphrinB2 treatment and glutamate stimulation potentiates CREB Ser¹³³ phosphorylation until at least DIV 7, suggesting that even as neurons mature, ephrinB2 treatment is capable of stimulating CREB phosphorylation. **(B)** Enhancement of CREB-dependent transcription. Neurons were transfected with reporter constructs, treated with ephrinB2-Fc or Fc followed by glutamate or control stimulation, and analyzed by the dual-luciferase reporter system. Luciferase activity is presented as fold induction over Fc and mock stimulation (NLU, normalized luciferase units). Neurons were also treated with D-APV (**P* < 0.01 versus Fc + glutamate treatment, ANOVA; *n* = 3). **(C and D)** Requirement of EphB cytoplasmic domain and Src family member activation. Neurons were transfected with luciferase constructs and pCDNA3, EphB2TR, or EphB2WT (C) or treated with control, PP2 (0.5 μ M), or PP3 (0.5 μ M) (D) and analyzed as in (B) (**P* < 0.01 versus Fc + glutamate treatment in each condition, ANOVA; *n* = 3). Glutamate stimulation led to a statistically significant increase in CRE-luciferase induction in all cases except for D-APV treatment.

suggest that ephrinB2 potentiates glutamate stimulation of Ca²⁺ influx through the NMDA receptor by inducing a Src family member, which in turn phosphorylates NR2B. The phosphorylation of NR2B then enhances the ability of the NMDA receptor to regulate the influx of Ca²⁺ in response to glutamate.

One function of ephrinB2 potentiation of glutamate-stimulated Ca²⁺ influx might be the activation of Ca²⁺-regulated immediate-early genes (IEGs) (3, 28, 29). NMDA receptor stimulation can induce IEG transcription by activating the Ca²⁺/cAMP-responsive element binding protein (CREB) through phosphorylation of CREB Ser¹³³ (3, 30). Therefore, we assessed whether exposure of neurons to ephrinB2 affected glutamate stimulation of CREB Ser¹³³ phosphorylation and CREB-dependent reporter-gene transcription.

Treatment of cells with ephrinB2-Fc or glutamate alone had little effect on the level of CREB Ser¹³³ phosphorylation or CREB-dependent reporter-gene expression (Fig. 4, A and B) (31). Treatment of neurons with ephrinB2-Fc, followed by glutamate stimulation, substantially increased CREB Ser¹³³ phosphorylation and reporter-gene transcription (Fig. 4, A and B). The effect of ephrinB2 is mediated by the NMDA receptor because treatment of neurons with D-APV blocked the effect of ephrinB2 (Fig. 4, A and B). EphB2TR, which blocks EphB signaling, or inhibition of Src family members with PP2 eliminated ephrinB2 potentiation of glutamate-stimulated gene expression (Fig. 4, C and D). These findings demonstrate that ephrinB2 potentiates CREB phosphorylation and activation by an EphB- and Src family-dependent mechanism.

REPORTS

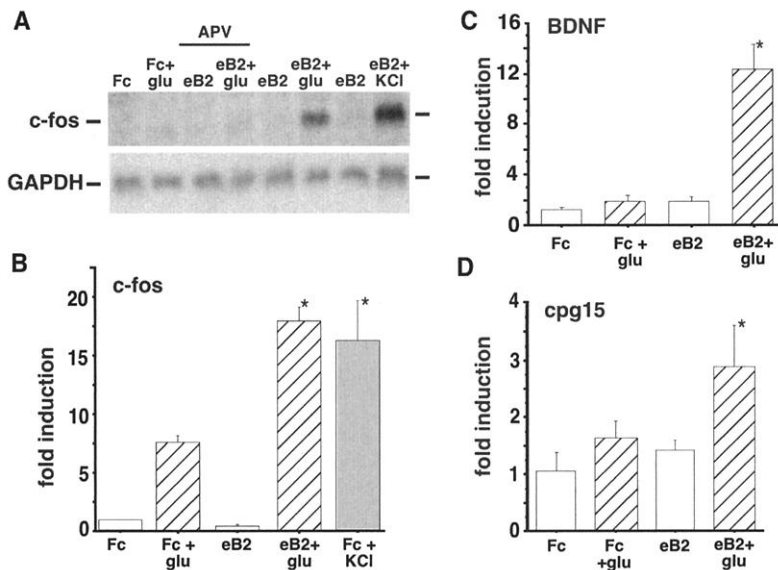


Fig. 5. EphB activation modulates Ca²⁺-dependent gene expression. (A) Analysis of *c-fos* expression in neurons (E18 + 2 to 3 DIV). Neurons were treated with ephrinB2-Fc or Fc for 45 min followed by stimulation with glutamate, 55 mM KCl, or control solution. RNA was collected and analyzed for *c-fos* mRNA expression (upper panel); the same blot was probed for *GAPDH* mRNA to control for loading (lower panel). (B) Effect of EphB activation on *c-fos* expression. Quantification of *c-fos* expression normalized to *GAPDH* after various treatments (**P* < 0.01 versus Fc + glutamate, ANOVA; *n* = 4). (C and D) Analysis of *BDNF* and *cpq15* mRNA in cortical neurons (E18 + 1 to 2 DIV for *BDNF* or 3 DIV for *cpq15*) that were first treated with Fc or ephrinB2-Fc, followed by glutamate stimulation (20 μM) for 4 hours. The level of *BDNF* or *cpq15* mRNA was determined by real-time PCR analysis (iCycler) and is presented as fold induction over Fc and mock stimulation (**P* < 0.01 versus Fc treatment, ANOVA; *n* = 3).

We next investigated whether ephrinB2 potentiates glutamate stimulation of specific IEGs that might regulate synapse formation, maturation, or function. Neurons were treated with ephrinB2 or control reagents for 45 min, then stimulated with glutamate or by membrane depolarization with elevated concentrations of KCl to stimulate the influx of Ca²⁺ through L-type voltage-sensitive Ca²⁺ channels (31). Glutamate-stimulated expression of *c-fos*, a transcription factor that mediates cellular responses to extracellular stimuli, was enhanced after activation of EphB (Fig. 5, A and B). The effect of ephrinB2 treatment on *c-fos* transcription is specific to NMDA receptor activation because the enhancement of *c-fos* expression was blocked by D-APV and the induction of *c-fos* expression by KCl stimulation was not affected by EphB activation (11). Treatment of neurons with ephrinB2 also potentiated glutamate activation of two other genes, *BDNF* and *cpq15*, that have been implicated in synapse development and/or function (Fig. 5, C and D) (32, 33).

Our findings suggest a model in which activity-independent cues may influence activity-dependent processes by potentiating or modulating gene expression during the specification, strengthening, and remodeling of synaptic connections. This model is supported by recent experiments with EphB2-deficient mice that show an *in vivo* role for EphB2 in activity-dependent plasticity (34, 35). As neurons ma-

ture and form functional contacts, the effect of glutamate on Ca²⁺-dependent gene expression is tightly controlled. EphrinB activation of EphB promotes the clustering of NMDA receptors, and the modulation of NMDA receptor by EphB may sensitize the neurons to the effects of glutamate. Glutamate then stimulates increased Ca²⁺ influx to trigger programs of gene expression that may affect synapse formation, maturation, and plasticity. Taken together, these observations suggest that the ephrinB–EphB–NMDA receptor interaction may represent an early step in the initiation of synapse formation or maturation and may potentiate the ability of the NMDA receptor to respond to activity-dependent signals from the extracellular milieu.

References and Notes

- L. C. Katz, C. J. Shatz, *Science* **274**, 1133 (1996).
- M. Constantine-Paton, H. T. Cline, *Curr. Opin. Neurobiol.* **8**, 139 (1998).
- A. Ghosh, M. E. Greenberg, *Science* **268**, 239 (1995).
- C. S. Goodman, M. Tessier-Lavigne, in *Molecular and Cellular Approaches to Neural Development*, W. M. Cowan, T. M. Jessell, S. L. Zipursky, Eds. (Oxford Univ. Press, New York, 1997), pp. 108–178.
- J. G. Flanagan, P. Vanderhaeghen, *Annu. Rev. Neurosci.* **21**, 309 (1998).
- R. Klein, *Curr. Opin. Cell Biol.* **13**, 196 (2001).
- R. Torres et al., *Neuron* **21**, 1453 (1998).
- M. Buchert et al., *J. Cell Biol.* **144**, 361 (1999).
- M. B. Dalva et al., *Cell* **103**, 945 (2000).
- Cortical neurons were dissociated and cultured, and for Ca²⁺ imaging, neurons were incubated with 1 μM fura-2-AM (Molecular Probes) and imaged as described in the supplementary materials (36). EphrinB2-Fc and Fc were clustered with anti-human Fc (50 ng/ml; Jackson

Laboratory, Bar Harbor, ME) and used at a concentration of 500 ng/ml to stimulate neurons. For Ca²⁺ imaging, cDNA constructs encoding EphB2WT, EphB2TR (9), or vector control (pCDNA3) and a construct encoding green fluorescent protein (GFP) to mark transfected cells were introduced into E18 neurons in suspension with Lipofectamine 2000 reagent (Gibco-BRL) as described (36).

- M. B. Dalva, M. A. Takasu, M. E. Greenberg, unpublished data.
- S. J. Holland, E. Peles, T. Pawson, J. Schlessinger, *Curr. Opin. Neurobiol.* **8**, 117 (1998).
- Y. T. Wang, M. W. Salter, *Nature* **369**, 233 (1994).
- L. F. Lau, R. L. Huganir, *J. Biol. Chem.* **270**, 20036 (1995).
- J. A. Rostas et al., *Proc. Natl. Acad. Sci. U.S.A.* **93**, 10452 (1996).
- K. Rosenblum, Y. Dudai, G. Richter-Levin, *Proc. Natl. Acad. Sci. U.S.A.* **93**, 10457 (1996).
- X. M. Yu, R. Askalan, G. J. Keil II, M. W. Salter, *Science* **275**, 674 (1997).
- M. Sheng, J. Cummings, L. A. Roldan, Y. N. Jan, L. Y. Jan, *Nature* **368**, 144 (1994).
- M. A. Takasu, M. B. Dalva, M. E. Greenberg, unpublished data.
- After treatment, cultured cortical neurons were lysed in RIPA buffer for immunoprecipitation and Western analysis as described (36). Details of plasmids, antibodies, and inhibitors are described in (36). At 0.5 μM, PP2, PP3, and SU6656 did not inhibit EphB2 kinase activity or tyrosine kinase activation in general. We also observed an increase in Src activity after ephrinB2 stimulation of cultured neurons when lysates were immunoprecipitated with anti-Src and immunoprecipitated proteins were monitored for Src autophosphorylation by incorporation of [³²P]ATP.
- T. Nakazawa et al., *J. Biol. Chem.* **276**, 693 (2001).
- C. Ellis et al., *Oncogene* **12**, 1727 (1996).
- A. H. Zisch, M. S. Kalo, L. D. Chong, E. B. Pasquale, *Oncogene* **16**, 2657 (1998).
- T. E. Krnicik, D. Shalloway, *Cell* **49**, 65 (1987).
- S. Y. Lin et al., *Brain Res. Mol. Brain Res.* **55**, 20 (1998).
- M. Di Luca et al., *Neuroreport* **12**, 1301 (2001).
- A. H. Zisch et al., *Oncogene* **19**, 177 (2000).
- A. J. Cole, D. W. Saffen, J. M. Baraban, P. F. Worley, *Nature* **340**, 474 (1989).
- H. Bading et al., *Neuroscience* **64**, 653 (1995).
- A. J. Shaywitz, M. E. Greenberg, *Annu. Rev. Biochem.* **68**, 821 (1999).
- Neurons were transfected at 3 DIV by Ca²⁺ phosphate precipitation with CRE-luciferase reporter construct and *Renilla* luciferase as a transfection control, and luciferase analysis was performed with the Dual Luciferase Reporter Assay System (Promega). For analysis of endogenous gene expression, Northern analysis for *c-fos* and real-time polymerase chain reaction (PCR) for *BDNF* and *cpq15* were done as described (36).
- M. M. Poo, *Nature Rev. Neurosci.* **2**, 24 (2001).
- E. Nedivi, G. Y. Wu, H. T. Cline, *Science* **281**, 1863 (1998).
- I. C. Grunwald et al., *Neuron* **32**, 1027 (2001).
- J. T. Henderson et al., *Neuron* **32**, 1041 (2001).
- Supplementary Web material is available on Science Online at www.sciencemag.org/cgi/content/full/1065983/DC1.
- We thank J. Bikoff, A. Brunet, R. Dolmetsch, J. Komhauser, M. Lin, M. Sahin, J. Zieg, and members of the Greenberg laboratory for their help and advice; W. Chen, A. Nigh, and A. West for establishment of real-time PCR; L. Hu for preparation of antibodies; P. Stein and M. Mishina for cDNA constructs; P. Scheiffele for advice on lipid-mediated neuronal transfections; T. Pawson and R. Klein for sharing results before publication; and J. Brugge, G. Corfas, and S. Thomas for helpful discussions. M.E.G. acknowledges the support of the F. M. Kirby Foundation to the Division of Neuroscience. Supported by grants from the National Institute of Neurological Diseases and Stroke (NS17512 and NS12651) (R.E.Z.), the Chiron Life Sciences Research Foundation and NRSA fellowships (M.B.D.), and grants from the National Institutes of Health (CA43855) and the Mental Retardation Research Center (HD18655) (M.E.G.).

4 September 2001; accepted 27 November 2001
 Published online 20 December 2001;
 10.1126/science.1065983
 Include this information when citing this paper.